RSC Advances

PAPER

Published on 06 July 2026

Cite this: *RSC Adv.*, 2026, **16**, 38221

Formation of hierarchical supramolecular microstructures from 6-*O*-alkylated α-cyclodextrin and their application to the selective extraction of long-chain unsaturated fatty acid esters

Haruya Ishida, [a] Shuhei Miyakawa, [b] Hajime Shigemitsu, [c] Kaori Fukuzawa [b] and Toshiyuki Kida *[ad]

Received 20th May 2026
Accepted 27th June 2026

DOI: 10.1039/d6ra04383f

rsc.li/rsc-advances

We successfully fabricated rhombic plate-like microstructures composed of layered assemblies of head-to-head supramolecular dimers of 6-*O*-methylated and 6-*O*-ethylated α-cyclodextrins (6-Me-α-CD and 6-Et-α-CD, respectively). 6-Me-α-CD selectively extracted methyl elaidate (*trans*) over methyl oleate (*cis*) in methanol *via* microstructure formation driven by inclusion complexation between the 6-Me-α-CD dimer and fatty acid esters, whereas 6-Et-α-CD exhibited the opposite selectivity. These results demonstrate that subtle modulation of the alkyl chain length at the 6-*O* position of α-CD enables reversal of *cis*/*trans* selectivity in supramolecular extraction behavior. The origin of this selectivity was further elucidated by theoretical calculations based on density functional theory (DFT) and fragment molecular orbital (FMO) interaction energy analysis.

Introduction

Supramolecular assemblies constructed through the self-assembly of molecular building blocks have attracted considerable attention across diverse fields, including materials science,[1,2] biotechnology[3,4] and environmental science.[5,6] Among these systems, supramolecular assemblies derived from macrocyclic host molecules such as cyclodextrins, calixarenes, pillar[n]arenes and cucurbit[n]urils have been extensively investigated in host-guest chemistry,[7] separation science,[8,9] analytical chemistry,[10] organic synthesis[11,12] and photochemistry[13,14] owing to their well-defined internal cavities that enable selective guest recognition and stabilization of reaction intermediates. Representative examples highlight the functional significance of confined supramolecular spaces. Manna *et al.* demonstrated that a hexameric resorcinarene capsule can stabilize reactive carbocationic intermediates, thereby enabling mild and selective Friedel–Crafts reactions within its confined cavity.[15] In another notable study, nonporous adaptive crystals of pillar[6]arene derivatives were shown to undergo guest-induced structural transformations, allowing selective adsorption of bromoalkane through distinct host-guest binding modes.[16] Furthermore, pillar[5]arene-incorporated metal–organic frameworks have recently emerged as supramolecular docking platforms that enable single-crystal structure determination of alkyl-bearing molecules, including natural products and drugs that are otherwise difficult to crystallize.[17]

Cyclodextrins (CDs) are well-known macrocyclic hosts that form inclusion complexes with a wide range of guest molecules in both aqueous[18] and organic media.[19] In the solid state, CDs typically adopt three characteristic assembly modes—cage-type, channel-type and layer-type assemblies—primarily formed through hydrogen bonding between the hydroxyl groups on the upper and lower rims of the CD rings and/or host-guest interactions.[20] Exploiting these assembly characteristics, a variety of CD-based supramolecular nano- and microstructures have been successfully fabricated.[21–25] For instance, Jiang *et al.* reported that β-CD forms head-to-head supramolecular dimers *via* intermolecular hydrogen bonding between secondary hydroxyl groups in water upon complexation with sodium dodecyl sulfate.[26] These dimers further assemble into higher-order architectures such as tubular structures and multilamellar vesicles.[27] Such studies clearly demonstrate that dimer formation can serve as a critical intermediate step in hierarchical CD-based self-assembly in water.

In this study, we focus on 6-*O*-alkylated CDs, specifically 6-*O*-methylated and 6-*O*-ethylated α-CD (6-Me-α-CD and 6-Et-α-CD, respectively), as molecular building blocks for constructing well-defined supramolecular architectures. These modified CDs

[a]*Department of Applied Chemistry, Graduate School of Engineering, The University of Osaka, 2-1 Yamada-oka, Suita, Osaka 565-0871, Japan*

[b]*Graduate School of Pharmaceutical Science, The University of Osaka, 1-6 Yamada-oka, Suita, Osaka 565-0871, Japan*

[c]*National Institute for Materials Science (NIMS), 1-2-1 Sengen, Tsukuba, Ibaraki 305-0047, Japan*

[d]*Integrated Frontier Research for Medical Science Division, Institute for Open and Transdisciplinary Research Initiatives (OTRI), The University of Osaka, 2-1 Yamada-oka, Suita, Osaka 565-0871, Japan. E-mail: kida@chem.eng.osaka-u.ac.jp*

are capable of forming head-to-head dimeric assemblies in organic solvents through intermolecular hydrogen bonding between the secondary hydroxyl groups, analogous to the behavior previously reported for 6-*O*-triisopropylsilylated β-CD.[28] We hypothesized that such preorganized dimeric units could undergo controlled secondary assembly to generate unique supramolecular microstructures. Herein, we report the fabrication of well-regulated rhombic plate-like supramolecular microstructures from 6-Me-α-CD and 6-Et-α-CD (Fig. 1), as well as their selective extraction behavior toward long-chain unsaturated fatty acid esters. The observed selectivity originates from inclusion complexation between fatty acid esters and the CD dimers, coupled with supramolecular microstructure formation. Notably, subtle modulation of the alkyl chain length at the 6-*O* position enables reversal of *cis*/*trans* selectivity. To the best of our knowledge, this work represents the first example of supramolecular structure formation achieved through controlled secondary assembly of supramolecular dimers derived from chemically modified CDs.

Experimental section

Hexakis(6-*O*-methyl)-α-CD (6-Me-α-CD) and hexakis(2,3-di-*O*-benzyl)-α-CD were purchased from Cyclodextrin-Shop (Netherlands). Hexakis(6-*O*-ethyl)-α-CD (6-Et-α-CD) was synthesized from hexakis(2,3-di-*O*-benzyl)-α-CD in two steps with reference to the reported method[29] (Schemes S1–3).

Preparation of supramolecular structures from 6-Me-α-CD

6-Me-α-CD (2.0 mg, 1.9×10^{-3} mmol), which was dried at 80 °C for 12 h *in vacuo* before use, was dissolved in methanol (1.0 mL) to prepare a 6-Me-α-CD/methanol solution (1.9 mmol L^{-1}). This solution (0.5 mL) was added dropwise to a poor solvent (1.0 mL) and stirred at 500 rpm at 25 °C for 24 h. The resulting precipitate was collected by centrifugation and subsequently dried under a nitrogen flow. The obtained solids were analyzed with powder X-ray diffraction (PXRD) and scanning electron microscopy (SEM).

Preparation of supramolecular structures from 6-Et-α-CD

6-Et-α-CD (5.0 mg, 4.4×10^{-3} mmol), which was dried at 80 °C for 12 h *in vacuo* before use, was dissolved in methanol (1.0 mL) to prepare a 6-Et-α-CD/methanol solution (4.4 mmol L^{-1}). This solution (0.2 mL) was added dropwise to a poor solvent (0.4 mL) and stirred at 500 rpm at 25 °C for 24 h. The resulting precipitate was collected by centrifugation and subsequently dried under a nitrogen flow. The obtained solids were analyzed with PXRD and SEM.

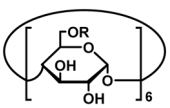

Fig. 1 Chemical structures of the 6-*O*-alkylated α-cyclodextrins.

Theoretical calculations

Energy-minimized structures of the inclusion complexes between the 6-*O*-alkylated α-CD dimers and the unsaturated fatty acid methyl esters (methyl elaidate and methyl oleate) were first explored by molecular mechanics calculations using the OPLS4 force field[30] in the gas phase. The framework of the 6-*O*-alkylated α-CD dimer used in these calculations was derived from the single-crystal X-ray structure of the 6-Me-α-CD dimer crystallized from a methanol/water/diethyl carbonate solution.[31] Initial host-guest geometries were generated by conformational sampling using the Mixed torsional/Low-mode sampling (MTLMOD) method, which efficiently explores both torsional degrees of freedom and large-scale low-frequency motions.[32] In this procedure, the placement of the unsaturated fatty acid methyl esters was systematically varied at several plausible binding sites of the α-CD dimer, including the primary-rim cavity and the internal space between the two α-CD units. These structures were employed as starting points for subsequent density functional theory (DFT) optimizations including solvent effects. From the resulting conformational ensemble, the three lowest-energy structures were selected and subsequently optimized by DFT calculations using the B3LYP-D_3 functional[33–35] with the 6-31G(d) basis set, as implemented in the Gaussian 16 program package.[36] Solvent effects were taken into account by employing the IEFPCM implicit solvation model[37] (methanol) during geometry optimization. The DFT-optimized structures were confirmed to have no imaginary frequencies, and the lowest-energy structure was taken as the representative inclusion complex. To further investigate the stability differences among the inclusion complexes, interaction energy analyses were performed for the optimized structures using the Fragment Molecular Orbital (FMO) method.[38,39] FMO calculations were carried out at the second-order Møller–Plesset perturbation theory (MP2) level[40,41] with the 6-31G(d) basis set, and inter-fragment interaction energy (IFIE) and Pair Interaction Energy Decomposition Analysis (PIEDA) were used to quantitatively evaluate the detailed host-guest interactions within the inclusion complexes.[42]

Results and discussion

Preparation of supramolecular structures from 6-*O*-alkylated α-CD

Supramolecular structures were prepared by adding a methanol solution of 6-*O*-alkylated α-CD dropwise into poor solvents such as hexane or cyclohexane, followed by standing at 25 °C for 24 h. The resulting precipitates were collected by filtration and dried under an N_2 flow prior to PXRD and SEM analyses.

Fig. 2A and B show SEM images of the precipitates obtained from mixtures of 6-Me-α-CD/methanol with hexane and cyclohexane as poor solvents, respectively. In both cases, rhombic microplates with lateral dimensions of 1–2 μm and thicknesses of 0.1–0.2 μm were observed. Fig. 2C shows the SEM image of

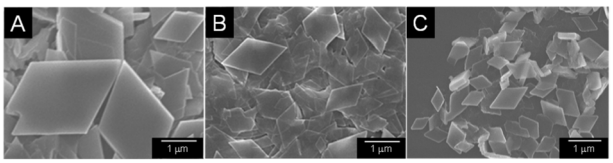

Fig. 2 SEM images of precipitates formed by dropwise addition of a 6-Me-α-CD/methanol solution into (A) hexane and (B) cyclohexane, followed by standing at 25 °C for 24 h. (C) SEM image of precipitates formed by adding a 6-Et-α-CD/methanol solution into hexane, followed by standing at 25 °C for 24 h.

the supramolecular structures formed from a combination of 6-Et-α-CD/methanol and hexane (a poor solvent). Similar rhombic microplates were observed; however, their lateral dimensions (0.2–0.5 μm) were clearly smaller than those observed for 6-Me-α-CD, whereas their thicknesses remained comparable (0.1–0.2 μm) (Fig. 2A), suggesting that the ethyl substituents may hinder crystal growth along the lateral direction compared with the methyl substituents.

The PXRD pattern of the rhombic microplates formed from 6-Me-α-CD in methanol/hexane is shown in Fig. 3A. Diffraction peaks were observed at $2\theta = 5.1°$, 7.6°, 10.2°, 12.9° and 19.9°. The reflections at $2\theta = 5.1°$ ($d = 17.4$ Å) and 10.2° ($d = 8.7$ Å) can be assigned to diffraction from the [001] and [002] planes of the head-to-head assembly of 6-Me-α-CD (Fig. 3D),[24] respectively, which is consistent with the formation of supramolecular dimers. Peaks at $2\theta = 7.6°$ [110], 12.9° [200] and 19.9° [310] are attributable to a laterally aligned hexagonal arrangement of the dimers (Fig. 3E).[43] The PXRD pattern of the rhombic microplates obtained from 6-Et-α-CD (Fig. 3C) was similar to that of 6-Me-α-CD, indicating comparable supramolecular packing. These results suggest that the rhombic plate-like microstructures are constructed from head-to-head supramolecular dimers of 6-Me-α-CD and 6-Et-α-CD, which are laterally organized into hexagonal arrays.

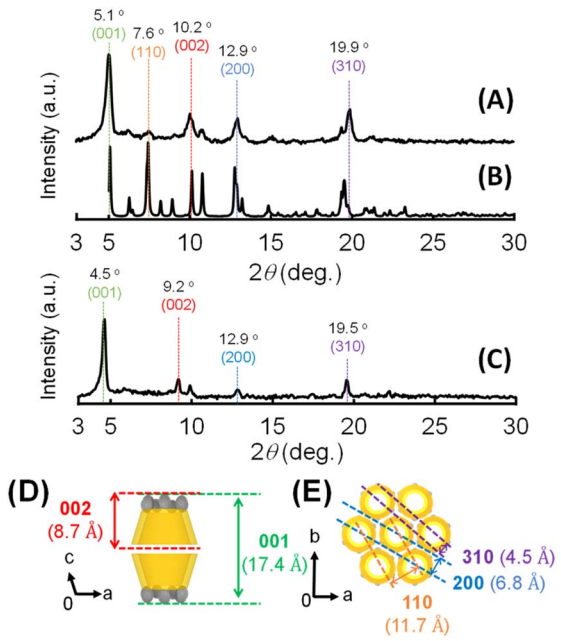

Fig. 3 (A) PXRD patterns of precipitates obtained by dropwise addition of a 6-Me-α-CD/methanol solution into hexane, followed by standing at 25 °C for 24 h. (B) Simulated PXRD pattern based on the single-crystal structure of 6-Me-α-CD obtained from a methanol/water/DEC system. (C) PXRD patterns of precipitates formed by dropwise addition of a 6-Et-α-CD/methanol solution into hexane followed by standing at 25 °C for 24 h. (D, E) Schematic illustrations of the (D) head-to-head arrangement and (E) lateral hexagonal packing of 6-Me-α-CD.

A single crystal of 6-Me-α-CD was obtained by standing a methanol/water/diethyl carbonate (DEC) solution of 6-Me-α-CD at 80 °C for one week. X-ray crystallographic analysis revealed that 6-Me-α-CD molecules form head-to-head dimers *via* intermolecular hydrogen bonding between the 3-OH groups, with an H···O distance of 2.16 Å (Fig. 4A and B).[31] These dimers further assemble into layered structures featuring a lateral hexagonal packing and a slightly offset vertical alignment (Fig. 4C and S7). The hexagonal arrangement is stabilized by intermolecular hydrogen bonding between the 2-OH groups of adjacent 6-Me-α-CD molecules, with an H···O distances of 1.86–1.95 Å (Fig. 4D). Although the molecules adopt locally hexagonal packing within each layer, the layered stacking is considered to induce anisotropic crystal growth. The resulting directional imbalance in growth suppresses the development of a hexagonal morphology and instead favors the formation of rhombic plate-like assemblies.[44]

The PXRD pattern simulated from the single-crystal data of 6-Me-α-CD (Fig. 3B) is consistent with the experimental PXRD pattern of the supramolecular structures formed from 6-Me-α-CD (Fig. 3A), indicating that the microstructures consist of layered assemblies of head-to-head supramolecular 6-Me-α-CD dimers.

We next investigated the formation of supramolecular structures from 6-*O*-alkylated α-CD by mixing its methanol

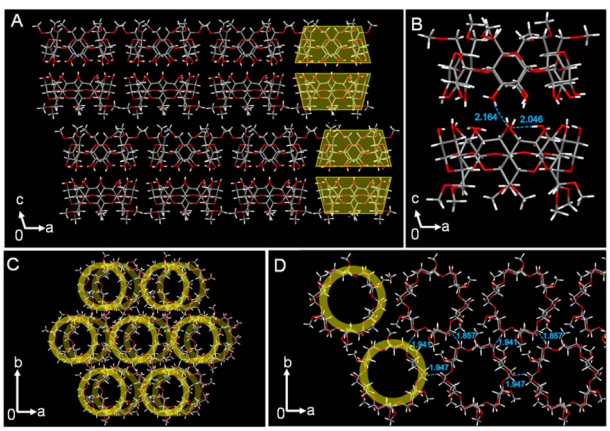

Fig. 4 Crystal structure of the 6-Me-α-CD assembly. (A and B) side views; (C and D) top views. 6-Me-α-CD molecules are displayed using a cylinder representation. Color labels: white, hydrogen; gray, carbon; red, oxygen. In (A), selected 6-Me-α-CD molecules are illustrated as yellow trapezoids, while in (C) and (D), selected 6-Me-α-CD molecules are shown as yellow circles. Darker yellow indicates the top-most layer. Methanol and DEC molecules are omitted for clarity.

solution with long-chain unsaturated fatty acid esters, such as methyl elaidate (*trans*) and methyl oleate (*cis*). These fatty acid esters can act not only as poor solvents but also as potential guest molecules for the CD. Rhombic supramolecular microplates were also obtained when either methyl elaidate or methyl oleate (0.33 μL, 9.7×10^{-4} mmol) was added dropwise to a methanol solution of 6-Me-α-CD (1.0 mL, 1.9 mmol L^{-1}) (Fig. 5). In both cases, the resulting microplates (lateral dimensions of 5–10 μm and thicknesses of 0.3–0.5 μm) were larger than those obtained when hexane or cyclohexane was used as the poor solvent, suggesting that these fatty acid esters enhance the supramolecular assembly process of 6-Me-α-CD, possibly by promoting the formation of 6-Me-α-CD dimers in methanol. Moreover, the yield of the microstructures was higher when methyl elaidate was used (1.6 mg) than when methyl oleate was employed (1.1 mg), although their sizes were comparable. This finding suggests that methyl elaidate more effectively promotes the formation of supramolecular structures than methyl oleate, possibly by enhancing the initial inclusion complex formation between the 6-Me-α-CD dimer and the fatty acid esters in methanol. PXRD and NMR analyses confirmed that these rhombic microplates are composed of a 1 : 1 inclusion complex between head-to-head supramolecular dimers of 6-*O*-alkylated α-CD and the fatty acid ester guests (Fig. S8, S11 and S12).

Selective extraction of unsaturated fatty acid esters

Based on the above-mentioned observations, we investigated the *cis*/*trans*-selective extraction of unsaturated fatty acid esters from an equimolar mixture of methyl elaidate and methyl oleate by utilizing the formation of inclusion complexes between the 6-*O*-alkylated α-CD dimers and the fatty acid esters, followed by their supramolecular assembly. After addition of a mixture of fatty acid esters (0.33 μL) to a methanol solution of 6-Me-α-CD (1.0 mL, 1.9 mmol L^{-1}), the resulting solution was stirred at 25 °C and then allowed to stand for 24 h, leading to the formation of rhombic microplates composed of supramolecular assemblies of the corresponding CD dimers (Fig. 6A, S9 and S10), similar to the results described above. The concentrations of the remaining fatty acid esters in the supernatant separated from the precipitate, were quantified by GC-MS to determine the extraction percentage of each ester. In this case, methyl elaidate was preferentially extracted into the supramolecular assemblies

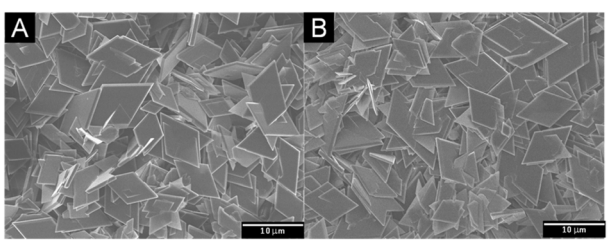

Fig. 5 (A and B) SEM images of precipitates obtained by dropwise addition of (A) methyl oleate and (B) methyl elaidate into a 6-Me-α-CD/methanol solution, followed by standing at 25 °C for 24 h.

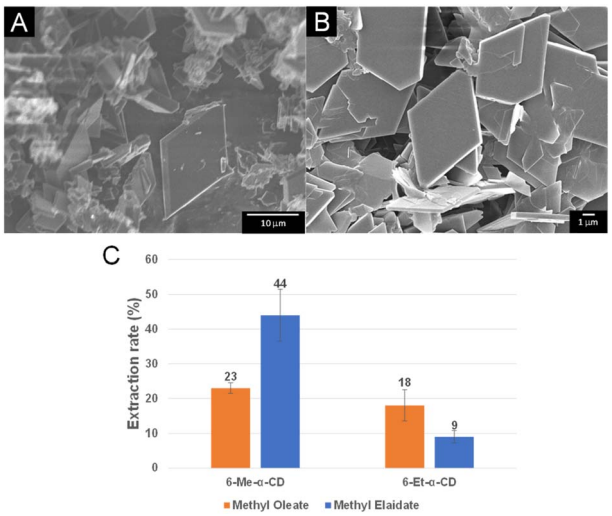

Fig. 6 (A and B) SEM images of precipitates obtained by dropwise addition of an equimolar mixture of methyl oleate and methyl elaidate into (A) a 6-Me-α-CD/methanol solution or (B) a 6-Et-α-CD/methanol solution, followed by standing at 25 °C for 24 h. (C) Extraction rates of methyl elaidate (blue) and methyl oleate (orange) in methanol through supramolecular structure formation induced by inclusion complexes between the 6-*O*-alkylated α-CD dimer and the fatty acid esters.

over methyl oleate, with an extraction amount approximately twice that of methyl oleate (Fig. 6C). Similarly, addition of a mixture of fatty acid esters (0.81 μL) to a methanol solution of 6-Et-α-CD under otherwise identical conditions yielded rhombic microplates as precipitates (Fig. 6B). In contrast, GC-MS analysis of the supernatant revealed that 6-Et-α-CD selectively extracted methyl oleate (Fig. 6C). These results demonstrate that the *cis*/*trans*-selective extraction of long-chain unsaturated fatty acid esters is achieved through a supramolecular assembly process driven by inclusion complex formation between 6-*O*-alkylated α-CD dimers and the fatty acid ester guests. Notably, modulation of the alkyl chain length at the 6-*O* position of α-CD enables a reversal of *cis*/*trans* selectivity in the supramolecular extraction behavior.

DFT-based evaluation of binding selectivity

To elucidate the origin of the *cis*/*trans*-selective extraction of long-chain unsaturated fatty acid esters through the supramolecular assembly process of 6-*O*-alkylated α-CD, density functional theory (DFT) calculations were performed to evaluate the optimized structures of the inclusion complexes between 6-*O*-alkylated α-CD dimers and the corresponding fatty acid ester guests, as well as their binding stabilization energies (Fig. 7A and B and Tables S1–S12). The optimized structures of the 6-Me-α-CD dimer complexes with methyl oleate and methyl elaidate revealed that the long alkyl chains of both fatty acid methyl esters were accommodated within the dimer cavity. The ester carbonyl group of each guest was positioned near the terminal methoxy groups of the dimer, suggesting attractive interactions that induce bending of the alkyl chain. A similar inclusion mode was observed for the 6-Et-α-CD dimer, in which the alkyl

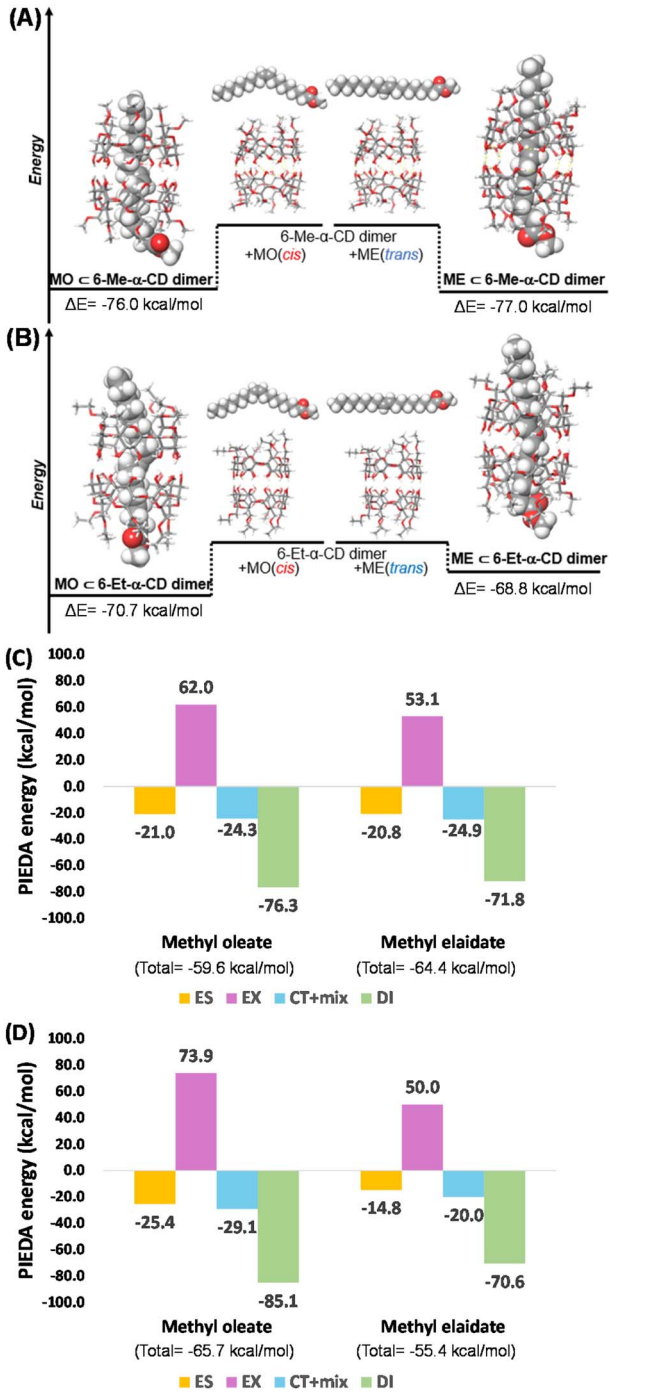

Fig. 7 (A and B) Energy diagrams for the complex formation of (A) the 6-Me-α-CD dimer with methyl oleate (MO) or methyl elaidate (ME) and (B) the 6-Et-α-CD dimer with MO or ME. Molecular sizes are not drawn to scale. (C and D) IFIE and PIEDA energy components for the interactions between the fatty acid esters and (C) 6-Me-α-CD and (D) 6-Et-α-CD. ES: electrostatic; EX: exchange-repulsion; CT + mix: charge-transfer plus mixed; DI: dispersion.

chains of the fatty acid esters were likewise encapsulated within the dimer cavity, while the ester carbonyl groups were located near the terminal ethoxy groups, leading to a bent molecular conformation. The calculated binding stabilization energy for the methyl elaidate/6-Me-α-CD dimer complex (−77.0 kcal mol^{-1}) was larger than that for the methyl oleate complex (−76.0 kcal mol^{-1}). In contrast, for the 6-Et-α-CD dimer, the stabilization energy of the methyl oleate complex (−70.7 kcal mol^{-1}) exceeded that of methyl elaidate (−68.8 kcal mol^{-1}), indicating stronger host-guest interactions between methyl oleate and the 6-Et-α-CD dimer. The stabilization energies of the fatty acid ester/6-Et-α-CD dimer complexes were lower than those of the corresponding 6-Me-α-CD dimer complexes. These results are consistent with the extraction behavior of unsaturated fatty acid esters mediated by the supramolecular assembly process of the 6-*O*-alkylated α-CDs, suggesting that the stability of the inclusion complexes between 6-*O*-alkylated α-CD dimers and fatty acid esters contributes to the selective extraction process. These contrasting trends in guest selectivity prompted further investigation into the underlying host-guest interaction mechanisms using interaction energy analysis based on the Fragment Molecular Orbital (FMO) method.

FMO interaction energy analysis

To further elucidate the differences in the stability of the inclusion complexes formed between each 6-*O*-alkylated α-CD dimer and the fatty acid methyl esters, we performed interaction energy analyses based on the Fragment Molecular Orbital (FMO) method[38,39] to investigate their host-guest interactions in detail. FMO calculations of inter-fragment interaction energy (IFIE) and Pair Interaction Energy Decomposition Analysis (PIEDA) were carried out for the inclusion complexes.[42] The results revealed substantial contributions from electrostatic (ES) and charge-transfer plus mixed (CT + mix) interactions, as well as from dispersion (DI) and exchange-repulsion (EX) interactions, between the 6-Me-α-CD dimer and the fatty acid esters (Fig. 7C and S13-16, Tables S13 and S14). Upon changing the guest from methyl elaidate to methyl oleate, the ES and CT + mix terms remained nearly unchanged, and the DI contribution slightly increased. In contrast, the EX interaction increased markedly, indicating enhanced steric repulsion arising from the bent alkyl chain of methyl oleate. This EX component originates from the overlap of electron densities between the host and guest molecules, reflecting steric repulsion caused by the close approach of atomic orbitals. In this CD dimer, the bent conformation of methyl oleate produced greater EX destabilization than the more linear methyl elaidate, rendering the latter guest intrinsically more favorable for inclusion. By comparison, in the case of the 6-Et-α-CD dimer, the DI with methyl oleate becomes stronger than that with methyl elaidate (Fig. 7D and S17–20, Tables S15 and S16). In addition, pronounced ES and CT + mix interactions between the terminal ethoxy groups (particularly fragments 7 and 11: Fig. S17 and S19) and the ester group of methyl oleate effectively compensate for the unfavorable contribution of EX. As a result, the inclusion complex with methyl oleate becomes more stable than that with methyl elaidate, leading to a reversal of selectivity. These results indicate that, in addition to the van der Waals interactions between the guest alkyl chain and the cavity wall of the dimer, electrostatic

interactions between the terminal alkoxy groups of the dimer and the ester carbonyl group of the guest also play an important role in stabilizing the inclusion complexes. The cooperative effect of these interactions contributes to the experimentally observed reversal of *cis*/*trans* selectivity upon varying the terminal alkyl substituent in the dimer.

Conclusions

In this study, we successfully fabricated rhombic plate-like microstructures composed of layered assemblies of head-to-head supramolecular dimers derived from 6-*O*-alkylated α-cyclodextrins (6-Me-α-CD and 6-Et-α-CD). These well-regulated microstructures were formed through the secondary assembly of supramolecular dimers in a mixed solvent system consisting of methanol and a poor solvent (serving as a guest), and this assembly process enabled the selective extraction of long-chain unsaturated fatty acid esters. Notably, 6-Me-α-CD preferentially extracted methyl elaidate (*trans*), whereas 6-Et-α-CD showed the opposite preference, selectively extracting methyl oleate (*cis*). This reversal of *cis*/*trans* selectivity demonstrates that subtle modulation of the alkyl substituent at the 6-*O* position of α-CD critically influences host-guest interactions within the dimer nanocavities. The origin of this selectivity was further elucidated by DFT calculations combined with FMO interaction energy analysis, which revealed that subtle differences in the balance of dispersion, electrostatic and exchange-repulsion interactions govern guest recognition within the dimer nanocavities. These findings highlight the utility of alkylated cyclodextrins as tunable supramolecular hosts capable of discriminating between structurally similar molecules through controlled dimer assembly and microstructure formation. The approach presented here offers a promising strategy for the selective separation of fatty acid esters and potentially other closely related organic compounds.

Author contributions

Toshiyuki Kida: conceptualization, supervision, project administration, funding acquisition, writing – review and editing. Haruya Ishida: investigation, formal analysis, visualization, writing – original draft. Hajime Shigemitsu: investigation, formal analysis, writing – review and editing. Shuhei Miyakawa: methodology, formal analysis, writing – review and editing. Kaori Fukuzawa: supervision, writing – review and editing.

Conflicts of interest

There are no conflicts to declare.

Data availability

All other data supporting this study are included in the supplementary information (SI). Ref. 30 and 32–42 are also cited in the SI, where they are renumbered 1–12.

CCDC 2512778 contains the supplementary crystallographic data for this paper.[31]

Supplementary information is available. See DOI: https://doi.org/10.1039/d6ra04383f.

Acknowledgements

This work was supported by a Grant-in-Aid for Scientific Research (No. 22H02146) from the Japan Society of the Promotion of Science and the OU Master Plan Implementation Project at The University of Osaka. The theoretical calculations were performed using the Fugaku supercomputer (project ID: hpci250154).

Notes and references

1 Y. Zhao, F. Sakai, L. SU, Y. Liu, K. Wei, G. Chen and M. Jiang, *Adv. Mater.*, 2013, **25**, 5215–5256.
2 R. Bleta, A. Ponchel and E. Monflier, *Environ. Chem. Lett.*, 2018, **16**, 1393–1413.
3 J. Zheng, C. Zhu, X. Xu, X. Wang and J. Fu, *J. Mater. Chem. B*, 2023, **11**, 6265–6289.
4 A. S. Mahadevi and G. N. Sastry, *Chem. Rev.*, 2013, **113**, 2100–2138.
5 W. Chen, P. Chen, G. Zhang, Y. Feng, Y.-W. Yang and L. Chen, *Chem. Soc. Rev.*, 2021, **50**, 11684–11714.
6 W.-H. Deng, X. Wang, K. Xiao, Y. Li, C. Liu, Z. Yao, L. Wang, Z. Cheng, Y. Lv, S. Xiang and Z. Zhang, *Chem. Eng. J.*, 2024, **497**, 154457.
7 T. Heinz, D. M. Rudkevich and J. Rebek Jr, *Nature*, 1998, **394**, 764–766.
8 J. Rebek Jr., *Acc. Chem. Res.*, 2009, **42**, 1660–1668.
9 P. Ballester, *Chem. Soc. Rev.*, 2010, **39**, 3810–3830.
10 W. Jian, D. Ajami and J. Jr. Rebek, *J. Am. Chem. Soc.*, 2012, **134**, 8070–8073.
11 T. S. Koblenz, J. Wassenaar and J. N. H. Reek, *Chem. Soc. Rev.*, 2008, **37**, 247–262.
12 M. Yoshizawa, J. K. Klosterman and M. Fujita, *Angew. Chem., Int. Ed. Engl.*, 2009, **48**, 3418–3438.
13 F. Hof, S. L. Craig, C. Nuckolls and J. Rebek Jr, *Angew. Chem., Int. Ed. Engl.*, 2002, **41**, 1488–1508.
14 M. Inouye, K. Hayashi, Y. Yonenaga, T. Itou, K. Fujimoto, T. U. M. Iwamura and K. Nozaki, *Angew. Chem., Int. Ed. Engl.*, 2014, **53**, 14392–14396.
15 P. La Manna, C. Talotta, G. Floresta, M. De Rosa, A. Soriente, A. Rescifina, C. Gaeta and P. Neri, *Angew. Chem., Int. Ed. Engl.*, 2018, **59**, 5423–5428.
16 J.-R. Wu, B. Li and Y.-W. Yang, *Angew. Chem., Int. Ed. Engl.*, 2020, **59**, 2251–2255.
17 Y. Wu, L. Shi, L. Xu, J. Ying, X. Miao, B. Hua, S. Chen, J. L. Sessler and F. Huang, *Nature*, 2005, **640**, 676–682.
18 M. V. Resharsky and Y. Inoue, *Chem. Rev.*, 1998, **98**, 1875–1918.
19 B. Siegel and R. Breslow, *J. Am. Chem. Soc.*, 1975, **97**, 6869–6870.
20 K. Harada, *Chem. Rev.*, 1998, **98**, 1803–1828.
21 H. Shigemitsu and T. Kida, *Polym. J.*, 2018, **50**, 541–550.
22 J. Wang and X. Zhang, *ACS Nano*, 2015, **9**, 11389–11397.

23 S. Uenuma, R. Maeda, H. Yokoyama and K. Ito, *Commun. Chem.*, 2019, **55**, 4158–4161.
24 T. Kida, A. Teragaki, J. M. Kalaw and H. Shigemitsu, *Commun. Chem.*, 2020, **56**, 7581–7584.
25 X. Hu, M. Shang, J. Wang, L. Liu, W. Lu, L. Ye and J. Wang, *ACS Appl. Bio Mater.*, 2021, **4**, 8033–8038.
26 L. Jiang, Y. Peng, Y. Yan and J. Huang, *Soft Mater.*, 2010, **6**, 1731–1736.
27 S. Yang, Y. Yan, J. Huang, A. V. Petukhov, L. M. J. Kroon-Batenburg, M. Drechsler, C. Zhou, M. Tu, S. Granick and L. Jiang, *Nat. Commun.*, 2017, **8**, 15856.
28 T. Kida, T. Iwamoto, H. Asahara, T. Hinoue and M. Akashi, *J. Am. Chem. Soc.*, 2013, **135**, 3371–3374.
29 K. Takeo, H. Mitoh and K. Uemura, *Carbohydr. Res.*, 1989, **187**(2), 203–221.
30 C. Lu, C. Wu, D. Ghoreishi, W. Chen, L. Wang, W. Damm, G. A. Ross, M. K. Dahlgren, E. Russell, C. D. Von Bargen, R. Abel, R. A. Friesner and E. D. Harder, *J. Chem. Theory Comput.*, 2021, **17**, 4291–4300.
31 CCDC 2512778: Experimental Crystal Structure Determination, 2026, DOI: 10.5517/ccdc.cq2qbrc6.
32 C. A. Parish, R. Lombardi, K. Sinclair, E. Smith, A. Goldberg, M. Rappleye and M. Dure, *J. Mol. Graphics Modell.*, 2002, **21**, 129–150.
33 A. D. Becke, *J. Phys. Chem.*, 1993, **98**, 5648–5652.
34 C. Lee, W. Yang and R. G. Parr, *Phys. Rev. B*, 1988, **37**, 785–789.
35 S. Grimme, J. Antony, S. Ehrlich and H. Krieg, *J. Phys. Chem.*, 2010, **132**, 154104.
36 M. J. Frisch, G. W. Trucks, H. B. Schlegel, G. E. Scuseria, M. A. Robb, J. R. Cheeseman, G. Scalmani, V. Barone, G. A. Petersson, H. Nakatsuji, X. Li, M. Caricato, A. V. Marenich, J. Bloino, B. G. Janesko, R. Gomperts, B. Mennucci, H. P. Hratchian, J. V. Ortiz, A. F. Izmaylov, J. L. Sonnenberg, D. Williams-Young, F. Ding, F. Lipparini, F. Egidi, J. Goings, B. Peng, A. Petrone, T. Henderson, D. Ranasinghe, V. G. Zakrzewski, J. Gao, N. Rega, G. Zheng, W. Liang, M. Hada, M. Ehara, K. Toyota, R. Fukuda, J. Hasegawa, M. Ishida, T. Nakajima, Y. Honda, O. Kitao, H. Nakai, T. Vreven, K. Throssell, J. A. Montgomery Jr, J. E. Peralta, F. Ogliaro, M. J. Bearpark, J. J. Heyd, E. N. Brothers, K. N. Kudin, V. N. Staroverov, T. A. Keith, R. Kobayashi, J. Normand, K. Raghavachari, A. P. Rendell, J. C. Burant, S. S. Iyengar, J. Tomasi, M. Cossi, J. M. Millam, M. Klene, C. Adamo, R. Cammi, J. W. Ochterski, R. L. Martin, K. Morokuma, O. Farkas, J. B. Foresman and D. J. Fox, *Gaussian 16, Revision C.01*, Gaussian, Inc., Wallingford CT, 2016.
37 G. Scalmani and M. J. Frisch, *J. Phys. Chem.*, 2010, **132**, 114110.
38 K. Kitaura, E. Ikeo, T. Asada, T. Nakano and M. Uebayasi, *Chem. Phys. Lett.*, 1999, **313**, 701–706.
39 Y. Mochizuki, S. Tanaka, K. Fukuzawa, *Recent Advances of the Fragment Molecular Orbital Method*, Springer, Berlin, Heidelberg, 2021.
40 Y. Mochizuki, T. Nakano, S. Koikegami, S. Tanimori, Y. Abe, U. Nagashima and K. Kitaura, *Theor. Chem. Acc.*, 2004, **112**, 442–452.
41 Y. Mochizuki, S. Koikegami, T. Nakano, S. Amari and K. Kitaura, *Chem. Phys. Lett.*, 2004, **396**, 473–479.
42 D. G. Fedorov and K. Kitaura, *J. Comput. Chem.*, 2007, **28**, 222–237.
43 J. M. Kalaw, H. Shigemitsu and T. Kida, *Langmuir*, 2022, **38**, 8407–8415.
44 E. Ringe, R. P. V. Duyne and L. D. Marks, *J. Phys. Chem. C*, 2013, **117**, 15859–15870.